Biogeochemistry
https://doi.org/10.1007/s10533-024-01124-4

Hourly methane and carbon dioxide fluxes from temperate ponds

Jonas Stage Sø · Kenneth Thorø Martinsen · Theis Kragh · Kaj Sand-Jensen

Received: 29 September 2023 / Accepted: 28 January 2024

Abstract Ponds are regarded as greenhouse gas (GHG) emission hot spots, but how hot are they? We examined this question by measuring methane (CH_4) and carbon dioxide (CO_2) fluxes in six forest and open land ponds on grasslands in Denmark during summer and winter. We used floating chambers with do-it-yourself sensors and automated headspace venting, allowing for 7404 hourly measurements. We found highly variable gas fluxes within ponds and between seasons and pond types. Ebullitive CH_4 fluxes were more variable than diffusive CH_4 fluxes. Ebullition was absent when total CH_4 fluxes were lowest (15 µmol m^{-2} h^{-1}), dominant (> 90%) at the highest fluxes (> 400 µmol m^{-2} h^{-1}), and increased with water temperature. In summer, a minor daily increase in diffusive fluxes was found on days with high wind speed, while CH_4 ebullition remained constant. CO_2 fluxes paralleled the day-night balance of photosynthesis and respiration. Mean CH_4 ebullition in open and forest ponds exceeded CH_4 diffusive fluxes 4.1 and 7.1-fold in summer (avg. 22.5 °C) and 2.3 and 2.5-fold in winter (9.6 °C), respectively. CO_2 emissions were higher on a molar basis than CH_4 emissions, both in summer and winter, while their annual global warming potentials were similar. Mean annual gas emissions from open and forest ponds (1092 and 2527 g CO_2e m^{-2} y^{-1}) are naturally high due to extensive external input of dissolved CO_2 and organic carbon relative to pond area and volume.

Keywords Ponds · Greenhouse gasses · Methane-CH_4 · Carbon dioxide-CO_2 · Diffusive flux · Ebullitive methane

Introduction

Methane (CH_4) and carbon dioxide (CO_2) fluxes are the two most important processes driving climate warming (Myhre & Shindell 2014), and lakes emerge as natural hot spots in the transmission of greenhouse gases (GHG; Rosentreter et al. 2021). Small lakes and ponds (< 5 ha) are globally abundant and have high fluxes relative to their areal cover, but these systems are poorly defined and often overlooked in investigations of GHG fluxes (Deemer et al. 2016; Richardson et al. 2022). Higher GHG fluxes in ponds, compared to larger lakes, may be due to the compounding

Supplementary Information The online version contains supplementary material available at https://doi.org/10.1007/s10533-024-01124-4.

Responsible Editor: Jack Brookshire.

J. S. Sø (✉) · T. Kragh
University of Southern Denmark, Campusvej 55, Odense M, 5230 Odense, Denmark
e-mail: jonassoe@biology.sdu.dk

K. T. Martinsen · K. Sand-Jensen
Freshwater Biological Laboratory, Department of Biology, University of Copenhagen, Universitetsparken 4, 3rd Floor, 2100 Copenhagen, Denmark

Published online: 08 March 2024

effects of higher organic substrate concentrations and higher temperatures (Deemer & Holgerson 2021). Ponds have a higher shoreline-to-surface-area ratio and, consequently, higher inputs of terrestrial organic material relative to surface area and water volume, causing high rates of degradation and production of CO_2 and CH_4 (Kuhn et al. 2021; Sand-Jensen & Staehr 2009). Furthermore, they receive substantial inputs of dissolved CH_4 and supersaturated CO_2 through sub-surface flow from the surroundings (Abril & Borges 2019; Striegl & Michmerhuizen 1998). As a result of large lateral inputs and internal production of organic material, pond sediments produce CO_2 and CH_4 which fuels the emission of GHG (Jansen et al. 2020b).

Goeckner et al. (2022) found differences in GHG emissions and carbon storage between natural and artificial ponds, with artificial ponds being carbon sources when younger (< 20 years), but carbon sinks when they become older (> 20 years). Moreover, surrounding land use and soil types may influence GHG fluxes (Peacock et al. 2021). Thus, despite only comprising 8.6% of the global lake area, small ponds (< 0.01 km^2) have been estimated to be responsible for approximately 40% of diffusive CH_4 emissions (i.e., 13.2–21.2 Tg CH_4 y^{-1}), according to early global estimates (Holgerson & Raymond 2016; Rosentreter et al. 2021). However, numbers and sizes of smaller ponds are difficult to assess using satellite imagery and include in the global GHG budget, resulting in large uncertainties of their contribution (Grinham et al. 2018).

CH_4 is formed by the degradation of organic substrates in the absence of oxygen and alternative electron acceptors (e.g., nitrate, ferric oxides and sulfate; Fenchel et al. 2012). The production is promoted by high rates of degradation at high temperatures and an ample supply of easily degradable organic substrates, when oxygen supply and alternative electron acceptors cannot metabolize the production of small organic acids (mainly acetate) and H_2 to CO_2 and H_2O (Fenchel et al. 2012). This situation may account for the observed increase in CH_4 fluxes and the CH_4:CO_2 flux ratio as lake size decreases, causing a higher warming potential per unit surface area (Holgerson & Raymond 2016; West et al. 2016). Hence, the higher input of organic substrates from external sources and in-lake production relative to surface area may increase CH_4 formation in small, typically warmer lakes during summer (Beaulieu et al. 2019; DelSontro et al. 2016). Although CH_4 and CO_2 emissions may be high from lakes and ponds, substantial carbon sequestration in the sediments will reduce net emission from the sites and downstream in the hydrological network (Anderson et al. 2014; Céréghino et al. 2014; Gilbert et al. 2021; Goeckner et al. 2022; Taylor et al. 2019). Thus, the debate of pond construction as a climate mitigation strategy should be evaluated as part of carbon budgets for the entire hydrological network at relevant time scales. Nonetheless, the debate of pond construction as a climate mitigation strategy remains unsettled.

The rates of microbial CH_4 production in sediments increase more with higher temperatures than CO_2 production, thereby increasing the CH_4:CO_2 flux ratio (Yvon-Durocher et al. 2014). In eight Swedish lake sediments, CH_4 production rates measured in incubations increased 10–100-fold between 4 and 20 °C and more strongly above 10 °C, though with considerable variation between lakes (Duc et al. 2010). The influence of temperature on CH_4 fluxes from lake surfaces is even more complex because CH_4 may be produced and oxidized by different aerobic and anaerobic processes in the sediment and the water column (Bogard et al. 2019; D'Ambrosio & Harrison 2021; Donis et al. 2017). Nonetheless, we expect substantially higher CH_4 production and fluxes during summer than winter, and particularly higher CH_4:CO_2 flux ratios as higher summer photosynthesis may reduce CO_2 emission (Jansen et al. 2020a; Wik et al. 2013, 2018, 2014).

A recent application of automated ventilated floating chambers deployed to 80 sites on a 10-ha lake revealed high spatial variability of CH_4 and CO_2 fluxes (Sø et al. 2023a, b). The chambers provided hourly diffusive and ebullitive fluxes throughout the diel cycle because the chamber headspace is automatically replenished with atmospheric air every hour allowing new measurements of gas fluxes between water and air. Sieczko et al. (2020) found that CH_4 fluxes from Swedish lakes were 2.4 times higher in the daytime than in the nighttime. This may be due to higher daytime wind speeds causing higher water column turbulence and sediment shear stress promoting CH_4 release from water and sediment surfaces (Joyce & Jewell 2003). When estimates of CH_4 fluxes are based solely on daytime measurements, this may lead to an overestimation of diel values (Sieczko et al.

2020). Floating chambers with automated headspace venting are suitable to test whether diel variations in CH_4 and CO_2 fluxes also are pronounced in ponds where wind speeds are markedly reduced due to sheltering by riparian vegetation, and short wind fetches (Vachon & Prairie 2013). CO_2 flux is likely lower during daytime due to photosynthesis and CO_2 consumption and higher during nighttime due to respiratory CO_2 release (Martinsen et al. 2022; Sand-Jensen et al. 2019). Measurements assessing variability of CO_2 and CH_4 fluxes within ponds are few.

Our goal was to determine CO_2 and CH_4 fluxes at high spatial and hourly resolution in six temperate ponds during summer and winter using automated floating chambers. To cover the two main types of small, nutrient-rich ponds, we examined three ponds located in a deciduous forest and three ponds located in open landscape nearby. We expect that forest ponds receive a higher input of organic matter that supports CO_2 and CH_4 effluxes. Ponds situated in open country receive higher summertime solar irradiance, are warmer and support higher in-pond primary production that, in turn, lowers CO_2 efflux. Overall, high input of organic matter and nutrient-rich conditions in both pond types may lead to profound CH_4 flux by diffusion and ebullition during both summer and winter.

Study sites and methods

This study was conducted during the winter and summer of 2022 in six shallow, nutrient-rich ponds located soil consisting of meltwater gravel and freshwater peat in North Zealand, Denmark (Fig. 1, Table 1). In some cases, sensors or batteries failed after a short time due to rough weather conditions; thus, data from two winter periods are included in the analyses of some ponds (Number of fluxes for each station is indicated on Fig. S2-4). Summer measurements were completed in late May or June, while winter measurements were done from January to the beginning of March. Three forest ponds (F1–F3, Table 1) and three are in open land nearby (O1–O3, Table 1) were studied. The area surrounding the forested ponds was dominated by old deciduous forest with few to no buildings. The forest is used for recreation and some timber production. The open land ponds were located in open grasslands, without

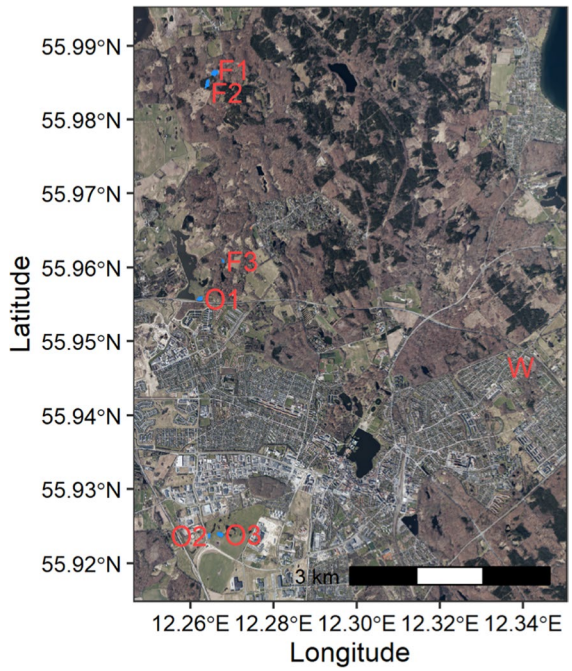

Fig. 1 Arial imagery of the ponds and weather station (W). Blue areas indicate the ponds

buildings but in urban transitions. The ponds vary in size (878–5897 m^2) and all experience substantial variations in water level. The age of the ponds varied, with two of the ponds (one in a forest and one open) being natural ponds of unknown age, whereas the rest were human-made ponds created 16–26 years ago to restore the natural hydrology or increase the biodiversity (Table S1). Water depth was measured in summer at the sites of GHG measurements. Four sites were selected for each pond, two in shallower waters (30–50 cm) and two in deeper waters (50–100 cm), whenever possible. One very deep pond (O2; 274 cm) was equipped with two additional floating chambers to cover the both shallow, intermediate and deep areas (Table 1). Distance between chamber positions ranged from 10 to 48 m.

Environmental conditions

Wind speed, gust and direction were measured one meter above the water surface in the middle of one forest pond (F1; HOBO S-WSB-M003 and HOBO S-WDA-M003, Onset, USA) and at a nearby public weather station (4–6 km from the ponds; Davis

Table 1 Overview of location and physiochemical conditions in three small forest ponds (F) and three small open ponds (O). LOI is the sediment organic content (mean (± SD) as % of dry mass) at the 4–6 sites of gas measurements

Pond	Latitude	Longitude	Size m^2	Age years	Min–max water depth of sites* cm	pH		Alkalinity		Total phosphorus		Total Nitrogen		Nitrate* µg N l^{-1}	Chlorophyll *a** µg l^{-1}	DOC mg C l^{-1}	Absorbance at 440 nm* cm^{-1}	LOI* %
						Winter	Summer	Winter	Summer	Winter	Summer	Winter	Summer					
								meq l^{-1}		µg P l^{-1}		µg N l^{-1}						
F1	55.9858012	12.2719778	5897	16–17	55–104	7.94	7.72	1.4	1.8	88	119	828	1266	13	27.6	17.9	0.0239	48.9 ± 24.2
F2	55.9846444	12.2700586	5041	16–17	65–98	7.5	8.27	1.0	1.2	110	87	1447	1286	7	8.4	15.8	0.0259	60.5 ± 8.95
F3	55.9605089	12.2716074	878	Natural	33–90	7.83	7.76	3.6	4.8	155	239	1619	1972	8	1.8	29.8	0.0511	66.3 ± 10.8
O1	55.9553805	12.2658086	3502	26	31–57	7.71	7.18	4.9	3.8	27	61	2028	929	5	24.5	13	0.0137	20.2 ± 2.37
O2	55.9233155	12.2651642	1789	17–18	154–274	7.25	7.85	0.6	1.1	83	67	1245	1063	143	30.2	10.1	0.0111	10.5 ± 5.90
O3	55.9234395	12.2676838	4314	Natural	43–59	8.05	9.87	5.3	1.7	120	236	2193	2700	6	5.4	35.7	0.0371	22.7 ± 1.56

*Summer values

Vantage Pro2, Lyngvig 2022). Wind speeds recorded at F1 were applied for the other two forest ponds, while public weather station data were used for all open ponds. Throughout the measuring period from 1 December 2021 to 30 July 2022, wind speeds in the forest remained lower than in open terrain. The barometric pressure was also acquired from the public weather station and used in Eq. 1 for all ponds. Each site was equipped with an oxygen and temperature sensor placed 50 cm above the sediment, when possible, and otherwise at the water surface. We measured temperature and oxygen in the pond water every 10 min (MiniDOT, PME, USA), while total phosphorus (TP), total nitrogen (TN) and dissolved organic carbon (DOC) were measured once during winter and summer following the methods of Kragh and Søndergaard (2004). TP and TN samples were stored at −18 °C. Upon analyses, the samples were acid-boiled in an autoclave and measured on a SKALAR autosampler. The DOC samples were filtered through a GF/F filter (Whatman, UK) and conserved using 2 M HCl. The water sample was later analyzed on a Shimadzu TOC (Shimadzu, Japan). Chlorophyll *a* and light absorbance of colored dissolved organic material (CDOM; Jespersen & Christoffersen 1987; Kirk 1994) were measured only during summer. Chlorophyll *a* was measured by ethanol extraction and spectrophotometric measurements of absorbance at 665 and 750 nm, while CDOM was measured as absorbance of 440 nm. The organic content of the upper 10 cm of sediment was measured in four cores (21 cm^2) for each pond in summer, with one core retrieved from each site within the 6 ponds and, thus, a total of 24 cores. The cores were split into two depth layers (0–5 cm and 5–10 cm) and the organic content was measured on duplicate samples as loss on ignition (LOI) at 550 °C. During winter, only one oxygen-temperature sensor remained in each pond. GHG measurements were not performed during the brief periods when the ponds were ice-covered which typically lasted less than one or two weeks. Submerged plant coverage in a plot of 2 × 2 m below the floating chambers was assessed visually during summer and categorized as: absent (0%), sparse (1–20%), high (20–90%), or complete coverage (90–100%). The most common submerged species present within the plot were *Callitriche* sp., *Ceratophyllum demersum*, *Chara* sp., *Elodea canadensis*, *Myriophyllum*

spicatum, *Potamogeton obtusifolius* and *Potamogeton pusillus.*

Automated floating chambers

Floating chambers contained electronic equipment that continuously measured CH_4 and CO_2 as described in Bastviken et al. (2015), modified to perform hourly measurements enabled by automated venting of the headspace by using an air pump (surface area: 0.0615 m^2, volume: 0.0135 m^3; Martinsen et al. 2018; Sø et al. 2023a, b). All measurements were done in 2022, with winter measurements performed in January and February and summer measurements between late May and June. CH_4, relative humidity, and temperature were measured every 2 s, while CO_2 was measured every 20 s. CH_4 and CO_2 fluxes were calculated by the use of small sensors (CH_4: NGM2611-E13, Figaro, USA, and CO_2: K33 ELG, SenseAir, Sweden) mounted in the air headspace within floating chambers that were placed on the sites. The CH_4 sensor was originally designed for high-concentration measurements, however, Bastviken et al. (2020) showed that using a new calibration and data processing technique the sensor can be used for CH_4 fluxes in floating chambers. The CH_4 sensor reacts to changes in absolute humidity, and thus measurements of relative humidity and temperature are needed to convert the voltage signal to CH_4 concentration. Data logging and the air pump were controlled by an Arduino (Arduino, Italy) which is equipped with a 10-bit analog-to-digital converter, which limits the resolution. We used a 10-point moving average, applied five times to increase the resolution of data, as proposed by Kajiura and Tokida (2021). The sensor precision is lower than commercialized laser equipment, which might cause difficulties in measuring low rates of change; we quantified this uncertainty in our measurements to 2.1 ± 2.1 and 3.4 ± 3.5 µmol CH_4 m^{-2} h^{-1} (see Sect. "Test of setup" below). Drift in the sensor has been shown to be within only 4–6 ppb per year for long-term measurements (Eugster et al. 2020), though this was not tested in our setup.

Each automated floating chamber measured CH_4 and CO_2 for a 40 min period, before a a small air pump was turned on for 20 min to ensure complete replenishment of headspace air with atmospheric air. Thus one measurement series was possible each hour (Sø et al. 2023a, b). The chamber had two hoses connected, one connected to the air pump, the other working as a pressure relief. The length and diameter (l: 1.5 m, Ø: 16 mm) of the hoses were tested to ensure no air would leave the chamber by diffusion. The air pump exchanged the air inside the chamber with atmospheric air, thus bringing the gas composition in the chambers close to that in the atmosphere and allowing continuous automated measurements of CH_4 and CO_2 fluxes. Chambers were tied to a sunk float that was held in place by an anchor, limiting the chambers to a one-meter float radius. All electronics were powered by an 18 Ah 4S $LiFePO_4$ battery floating next to the chamber. All sensors were turned on for a minimum of one hour before deployment, enabling the CH_4 sensor to warm up. Four chambers were distributed evenly between shallow and deep parts of each pond in areas without emergent vegetation.

Calibration of the gas sensors followed the procedure by Bastviken et al. (2020) and Sø et al. (2023a, b). All CH_4 sensors were calibrated individually, as the sensors do not react the same to changing humidity and CH_4 concentrations. During the calibration of the CH_4 sensors, a Gasmet DX4030 FTIR Gas Analyzer (Version E1.22) and an Ultraportable Greenhouse Gas Analyzer (Los Gatos Research, USA) were used. The two CH_4 analyzers were calibrated using standard CH_4 gases (100 ppm).

CH_4 and CO_2 fluxes

Each flux measurement of CH_4 was partitioned into ebullitive ($F_{CH4\text{-}ebul}$) and diffusive fluxes ($F_{CH4\text{-}diff}$), with their sum being the total flux ($F_{CH4\text{-}total}$). Thus for each flux measurement, both $F_{CH4\text{-}ebul}$ and $F_{CH4\text{-}diff}$ could be calculated. Flux of CO_2 (F_{CO2}) only occurred by diffusion due to the high solubility of CO_2 in water. All fluxes (µmol m^{-2} h^{-1}) were calculated using Eq. (1).

$$F = \frac{dC}{dt}\frac{P_{amb}V}{R_{gas}TA} \quad (1)$$

The first term (dC dt^{-1}) is the rate of change (µmol mol^{-1} h^{-1}) in the headspace of the chamber, P_{amb} is the ambient pressure (Pa.), V is the chamber volume (m^3), R_{gas} is the ideal gas constant (m^3 Pa K^{-1} mol^{-1}), T is the ambient temperature (K), and A is the surface area (m^2) of the floating chamber.

Positive fluxes indicate the gas leaving the water (source), whereas negative fluxes indicate the gas entering the water (sink).

Partitioning of $F_{CH4\text{-}ebul}$ and $F_{CH4\text{-}diff}$ was done according to Sø et al. (2023a, b). Specifically, ebullition events were characterized as a sudden increase in the headspace CH_4 concentration (Fig. 2). Ebullitive events were identified by computing a 5-point running variance as sudden changes in concentration result in high variance, whereas $F_{CH4\text{-}diff}$ is characterized by low variance. We determined a cutoff value for the running variance by visually identifying ebullitive events and the running variance. All measurements which exceeded the running variance cutoff value were classified as ebullitive measurements. We determined the minimum and maximum concentration within this period and calculated $F_{CH4\text{-}ebul}$ as the difference between maximum and minimum concentration. All measurements one minute before and after the event were also included in the ebullitive event, to encompass the entire concentration change caused by an ebullitive event. Additionally, a diffusive threshold value was applied to exclude changes less than 1 ppm from being regarded as ebullitive events.

$F_{CH4\text{-}diff}$ was calculated after the initial 200 measurements (6.5 min), i.e., the deadband, following the replacement of the chamber air, to avoid any initial instability, caused by large changes in humidity within the chamber which affects the CH_4 sensor measurements. Ebullition was not determined either during this period. The next 400 measuring points (13 min) were used to calculate the slope (dC/dt in Eq. 1), using a linear regression model. If ebullitive events occurred during the 400 measuring points, only the points before the ebullitive event were used. Models with a well-defined linear fit (i.e., an R^2 higher than 0.5 and more than 50 observations) were kept for calculation of $F_{CH4\text{-}diff}$, while the others were discarded. All $F_{CH4\text{-}diff}$ were visually inspected to ensure that the headspace concentration did not approach saturation resulting in a lower slope. $F_{CH4\text{-}ebul}$ was calculated for the entire period after the initial 6.5 min.

F_{CO2} was calculated on all measuring points of each measurement period, resulting in approximately 120 measurement points over 40 min. The CO_2 concentration in the chamber during the 40 min did not show any signs of saturation. A linear model was fitted for every 40 min period for each sensor. Models with an R^2 higher than 0.5 and more than 50 observations were retained, and the rest were discarded.

In all, 1390 measurements of $F_{CH4\text{-}diff}$ and 2701 $F_{CH4\text{-}ebul}$ were collected during summer and 1569 $F_{CH4\text{-}diff}$ and 4588 $F_{CH4\text{-}ebul}$ measurements in winter. There were 1942 hourly CO_2 fluxes in summer and 1009 in winter. The number of days with flux measurements averaged 21, 51, and 21 days per pond

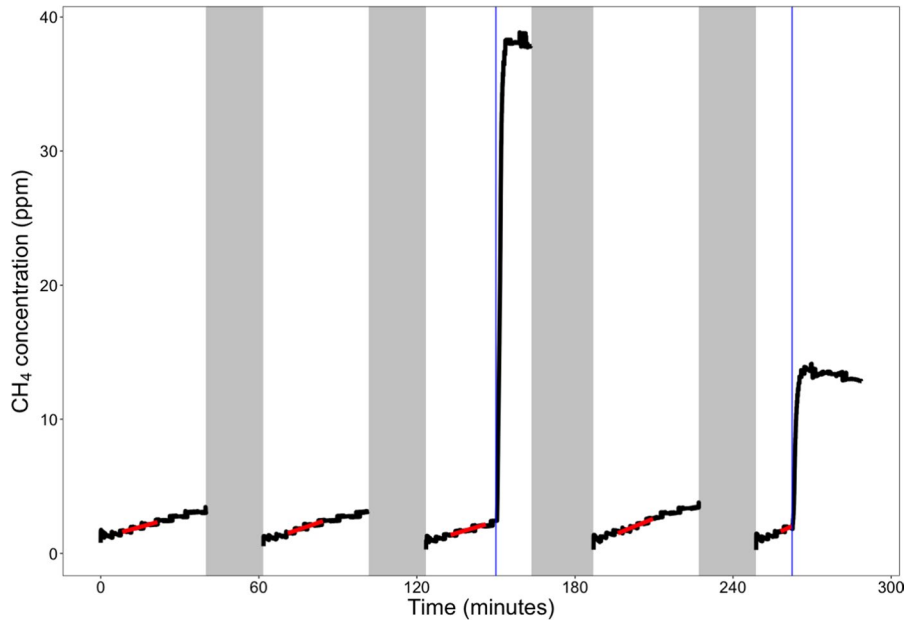

Fig. 2 Raw data from one sensor, with black dots indicating the raw data and grey areas indicating areas of flushing the chamber air. Red lines indicate the linear model in which the slope was used to determine the diffusive exchange rates. Sudden changes in concentration were considered ebullitive events, which are shown by vertical blue lines

of continuous hourly measurements of $F_{CH4\text{-}diff}$, $F_{CH4\text{-}ebul}$, and F_{CO2}, respectively. The large difference in available flux measurements is due to diffusive fluxes of CH_4 and CO_2 having R^2 values lower than 0.5 that were discarded.

The total GHG emission from the lake was calculated in terms of CO_2-equivalents (CO_2e) using the conversion of 27.2 as the global warming potential for non-fossil CH_4 for a time period of 100 years (IPCC 2022). The annual emissions of CO_2 and CH_4 were estimated as the mean of summer and winter fluxes.

Test of setup

The uncertainty of our setup was tested on two floating chambers, which were deployed in an open container filled with tap water at a depth of 20 cm. The container was initially equipped with two air pumps to ensure equilibrium in partial pressure of CH_4 between the atmosphere and the water. The container was open and exposed to natural weather conditions. Furthermore, to mimic higher piston velocity, a water circulation pump was turned on after 24 h. As anticipated, increasing piston velocity did not affect fluxes in this experimental situation with equilibrium in partial pressure between the water and the gas space. A total of 83 fluxes were measured with the two floating chamber sensors. Only 5% of the fluxes had an R^2 above 0.5, and 39% of the calculated fluxes were negative and 61% were positive. We assumed that no CH_4 formation would take place in the container, and expected no CH_4 flux between the water and the headspace in the chambers. The mean fluxes ($\pm$95% confidence intervals) for the two sensors were low, close to and not significantly different from zero (i.e., 1.9 ± 2.1 and 4.8 ± 3.5 µmol m^{-2} h^{-1}). Notably, under conditions with very high temperatures inside the chamber (> 35 °C) the CH_4 sensor may need longer time (> 15 min) to stabilize, due to rapid changes in absolute humidity.

Calculations of fluxes are difficult, even with high-precision equipment. This is further complicated by the low-resolution analog-to-digital converters used here. The signal-to-noise ratio is not proportional: the noise has a larger impact in situations with low fluxes. Thus, at low fluxes, linear estimation of the concentration change over time is difficult and may results in poor model estimates, causing a bias towards higher fluxes with accepted $R^2 > 0.5$ (Lammirato et al. 2017). This phenomenon was also noticeable in our dataset, which showed a similar inverse relationship between the diffusive fluxes of CH_4 and R^2 (Fig. S1).

Statistical analysis

Linear mixed models (LME) were used to determine the variables influencing $F_{CH4\text{-}ebul}$, $F_{CH4\text{-}diff}$, and F_{CO2}. Prior to any statistical modeling, all variables were examined for intercorrelation using Spearman rank correlation. An arbitrary Spearman ρ range between −0.39 and 0.39 was treated as uncorrelated and kept for analysis. Only one variable was kept if the ρ value was not within this range. Due to the large number of observations, the p-value was a poor measure of significance and was thus disregarded. To ease the interpretation of the model parameter estimates, all predictor variables were centered and scaled by subtracting the mean and dividing by the standard deviation, resulting in the same unit for all predictor variables. Sediment organic content (LOI) variables at 0–5 cm and 5–10 cm, DOC, and CDOM were found to be intercorrelated; LOI at 0–5 cm was retained for modeling.

Models were fitted using either hourly or average daily values of $F_{CH4\text{-}ebul}$, $F_{CH4\text{-}diff}$, and F_{CO2} as the response variable. As predictor variables, all models consisted of average water temperature, LOI, water depth, and plant coverage. Additionally, $F_{CH4\text{-}ebul}$ was used as a predictor variable in both models of $F_{CH4\text{-}diff}$. For the modeling using daily values, all predictor variables were also averaged. Model selection was performed using a stepwise backward elimination approach, removing predictor variables that were not significant until all remaining variables were significant (using likelihood ratio tests, $p < 0.05$). LME were used to account for the hierarchical nesting of the data, using sites nested within a pond as the random effects. An additional LME was created to determine if meteorological variables affected the ratio of ebullitive to total fluxes. This was done using the data from the public weather station. The model consisted of daily mean pressure, air temperature, and wind speeds. However, as seasonal differences in temperature and wind speeds can be large, we also created two models examining the meteorological variables' effect for each season. As previous results have shown differences in pond GHG fluxes based on them being artificial or natural, we created three LME

with $F_{CH4\text{-}diff}$, $F_{CH4\text{-}ebu}$, F_{CO2} as the dependent variables, respectively, and type (natural vs artificial) as the independent variable. To account for differences between ponds, we used pond as a random effect. For all models, the goodness of fit was assessed using the marginal (R^2_{marg}, fixed effects only) and conditional (R^2_{cond}, fixed and random effects) R^2.

We further used LMEs to determine differences in fluxes between forest and open ponds. $F_{CH4\text{-}ebul}$, $F_{CH4\text{-}diff}$, and F_{CO2} were used as dependent variables, and type (forest vs. open) and season were used as independent variables; season was included to take into account that some of the ponds had a higher number of fluxes available.

Diel variability of GHG-flux was assessed by generalized additive mixed modeling (GAMM) for each type of flux. The relationship between fluxes (response variables) and hour of the day (predictor) were modeled using cyclic cubic spline smoothing, which was evaluated for forest and open ponds during summer and winter. Moreover, ponds and sites within ponds were incorporated to account for nested data, similar to the linear mixed models. Significant diel correlation found in GAMM models was hypothesized to be due to variable wind speeds. Thus, ponds with diel variation in fluxes were modeled with wind speeds using LME. In the models, each flux was used as a response variable and wind speed from that type of pond was used as a predictor variable; we accounted for the nestedness of data like in the previous models.

Spatiotemporal variability was examined between sites within ponds and between types of ponds (forest and open) by calculating the coefficient of variation of the daily average fluxes, described as the standard deviation divided by the mean.

All data analysis and statistics were made using R (R Core Team 2018). For the linear mixed effects model, the *lme4* package was used (Bates et al. 2015), while the *mgcv* package was used for GAMM models (Wood 2011). R^2_{marg} and R^2_{cond} were calculated using the *MuMIn* package (Bartoń, 2018).

Results

Environmental conditions

All six ponds were alkaline, eutrophic, high in DOC, variable pH and with no systematic differences in water chemistry between forest and open ponds (Table 1). On average, the sediment organic contents at the 4–6 measuring sites in each pond were significantly higher in forest ponds (48.9–66.3%) than in open ponds (10.5–22.7%; t-test: df = 4, t = 6, $p = 0.04$). During gas flux measurements, mean water temperatures were slightly higher in open ponds than in forest ponds during both summer (23.8 and 21.1 °C, respectively) and winter (9.9 and 9.4 °C, Table 2). Two forest ponds had winter periods of hypoxia (< 10% oxygen saturation), while the other ponds were close to air saturation (Table S1). During summer, most pond sites had oxygen concentrations above air saturation during daytime and below during nighttime, but several high-plant-coverage sites in open ponds were permanently supersaturated (Table S1). One open pond (O3) had no submerged plants, while all forest ponds and one open pond (O1) had variable coverage between sites (ranging from no to high coverage) and another (O2) had full coverage (Table S1). Atmospheric pressure measurements were collected from the local weather station, showing on average a 1% difference in daily pressure from maximum to minimum, with higher average values during winter (1.3%, range: 0.2–3.1%) compared to summer (0.5%, range: 0.1–1%). The LME showed no significant relationship between $F_{CH4\text{-}diff}$, $F_{CH4\text{-}ebu}$, F_{CO2} and type (natural or artificial) of pond, indicating no differences in fluxes between natural and artificial ponds.

CH_4 flux

CH_4 flux took place by diffusion ($F_{CH4\text{-}diff}$) and ebullition ($F_{CH4\text{-}ebul}$). $F_{CH4\text{-}diff}$ was usually lower than $F_{CH4\text{-}ebul}$ and occasionally negative, indicating diffusive uptake from the atmosphere (Fig. 3, Table 2 and Fig. S5). 13% of the diffusive fluxes showed negative values; however, the median of these values was low at -25 µmol CH_4 m^{-2} h^{-1}. $F_{CH4\text{-}diff}$ was higher in forest ponds than open ponds in both summer (range: 58–156 *versus* 31–53 µmol m^{-2} h^{-1}, respectively) and winter (47–57 *versus* 23–29 µmol m^{-2} h^{-1}). $F_{CH4\text{-}diff}$

Table 2 Mean daily emissions of CH_4 (ebullitive and diffusive) and CO_2 of three forest and three open ponds in summer and winter

Season	Type	Daily temperature range	Average daily temperature	CH4-ebullition	CH_4-diffusion	CO_2-diffusion	CH_4 ebul:diff	CO_2:CH_4-total	CO_2:CH_4-total	CO_2+CH_4-total*
		°C	°C	mmol m^{-2} d^{-1}	mmol m^{-2} d^{-1}	mmol m^{-2} d^{-1}		mol:mol	GWP:GWP	g CO_2e m^{-2} y^{-1}
Summer	Forest	18.6–25.3	21.1	12.6 (2.5)	2.46 (0.29)	82 (12.4)	5.1	5.5	0.55	2453
	Open	20–26.2	23.8	4.29 (0.62)	0.95 (0.09)	29 (19.6)	4.5	5.5	0.56	911
Winter	Forest	4.3–12.5	9.4	1.25 (0.27)	1.24 (0.13)	49 (8.9)	1.0	19.8	2.0	
	Open	6–14.6	9.9	0.73 (0.29)	0.63 (0.06)	19 (8.9)	1.2	13.9	1.4	
Sum.:Wint	Forest			10.1	2.0	1.7				
	Open			5.9	1.5	1.5				

*Total annual emissions were estimated as the mean of summer and winter values

The ratios between emissions in summer and winter, ebullitive and diffusive CH_4 emissions, warming potential (GWP) of CO_2 relative to CH_4 emissions and total CO_2e-emissions are shown together with temperature ranges. Warming potential of CH_4 is set at 27.2 relative to CO_2. Standard error of the mean (SEM) is in parenthesis

was significantly higher in forest ponds compared to open ponds (estimate: 47.7 µmol m^{-2} h^{-1}, df = 4, t value = 4.9, $p = 0.007$).

$F_{CH4\text{-}ebul}$ varied extensively, both between sites within ponds and between ponds, and the variability was much higher than the variability of $F_{CH4\text{-}diff}$ and F_{CO2} (Fig. 3 and Table S2). Mean summer $F_{CH4\text{-}ebul}$ greatly exceeded winter $F_{CH4\text{-}ebul}$, however, this was not significant (range: 104–1162 *versus* 32–118 µmol m^{-2} h^{-1}, paired t-test: t = 2.1, df = 5, *p*-value = 0.09), and forest ponds had higher mean $F_{CH4\text{-}ebul}$ than open ponds (range: 62–441 *versus* 71–126 µmol m^{-2} h^{-1}), but this difference was not significant (df = 4, t value = 1.4, $p = 0.25$). Higher rates of $F_{CH4\text{-}ebul}$ are reflected by ebullition events in 69% of the measurements in forest ponds in summer and 21% in winter, compared with 54% and 17% in open ponds during the two seasons (Fig. 4).

In summer, $F_{CH4\text{-}diff}$ was significantly higher around noon than during nighttime in forest ponds (GAMM, edf = 1.6, F = 4.5, $p = 0.004$) and showed a tendency towards higher fluxes around 6 in the morning in open ponds (GAMM, edf = 1.2, F = 1.5, $p = 0.08$; Fig. 5). Only forest ponds showed a significant diel pattern during winter, with highest fluxes in the evening around 18 (GAMM, edf = 2, F = 72, $p < 0.001$). Diel variation in wind speeds were measured in open and forest ponds during summer, which were significantly related to $F_{CH4\text{-}diff}$ (LME, estimate 15.4 µmol CH_4 m^{-2} h^{-1} (m s^{-1})$^{-1}$, df = 4272, $p < 0.001$), showing higher $F_{CH4\text{-}diff}$ with increasing wind speeds (Fig. 5 and S2), however, during winter, wind speed correlated negatively to $F_{CH4\text{-}diff}$ (LME, estimate −3.2, df = 6189, $p = 0.01$). Forest ponds showed significant diel changes of $F_{CH4\text{-}ebul}$, during winter (GAMM, edf = 1.7, F = 13, $p < 0.001$), peaking at around noon. Similarly to $F_{CH4\text{-}diff}$, one LME showed a tendency in wind speeds towards $F_{CH4\text{-}ebul}$ (LME, estimate −7.1 µmol CH_4 m^{-2} h^{-1} (m s^{-1})$^{-1}$, df = 6642, $p = 0.06$); however, the estimate was negative, indicating higher ebullitive fluxes during periods of low wind speed.

High $F_{CH4\text{-}total}$ was primarily due to ebullition, as seen in comparisons between days, sites, ponds, and seasons (Fig. 4). No ebullition took place when $F_{CH4\text{-}total}$ was at the lowest level (15.5 µmol m^{-2} h^{-1}), and the percentage of ebullition in $F_{CH4\text{-}total}$ increased with higher $F_{CH4\text{-}total}$, attaining a maximum of 94%, and an asymptote of 90% at approximately 400

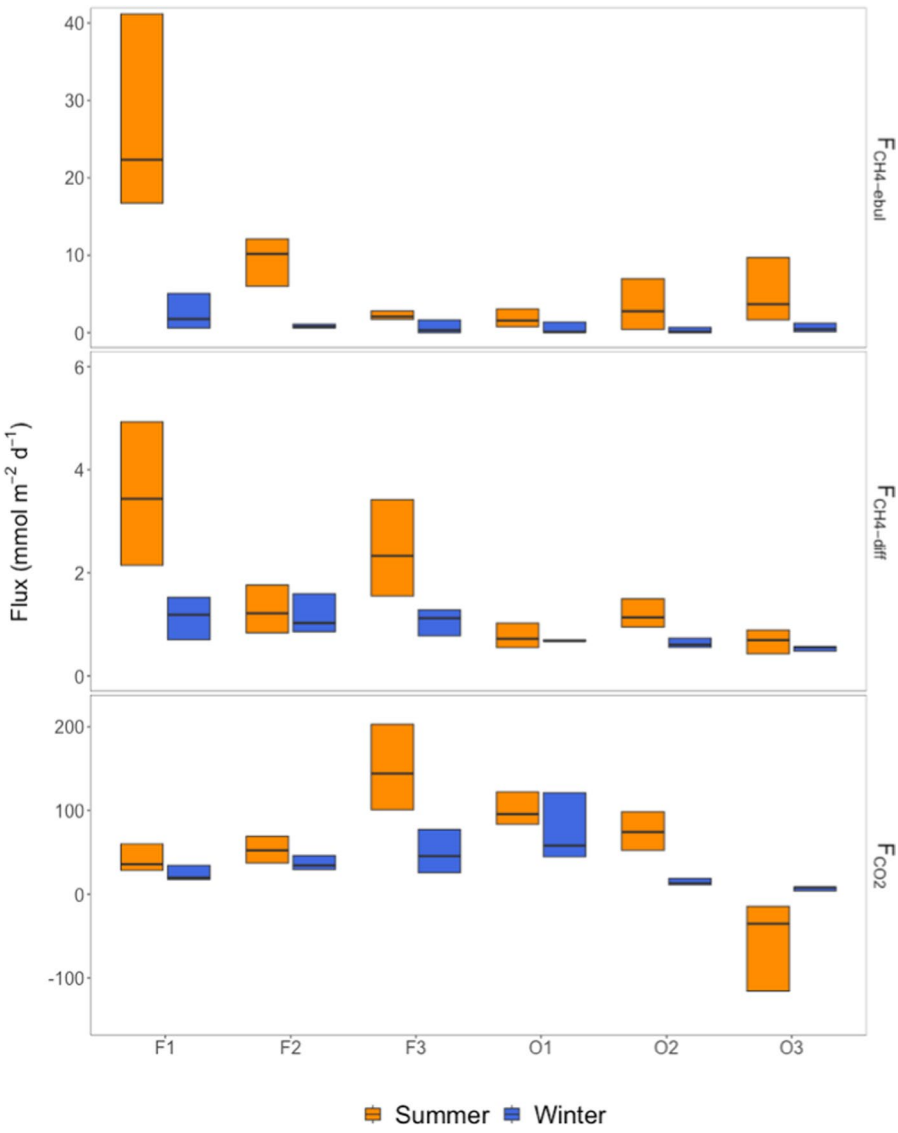

Fig. 3 Average daily fluxes of ebullitive and diffusive CH_4 and CO_2 of each pond during summer and winter. The solid horizontal line indicates the median, upper and lower hinges indicate the 25th and 75th quartile

μmol m^{-2} h^{-1}. The LME containing air temperature, atmospheric pressure, and wind speeds showed a significant relationship with the daily average proportion of ebullition, with an R^2_{marg} of 0.23 and an R^2_{cond} of 0.6 when including all the data. When examining the relationship for each season, no meteorological variables had significant influence.

CO_2 flux

F_{CO2} showed substantial variation between ponds (Figs. 3 and S5), however, no significant differences were found between forest and open ponds (df = 4, t value = 0.63, $p = 0.57$). Summer mean values of forest ponds ranged from 1786 to 6508 μmol CO_2 m^{-2} h^{-1}, while lower fluxes in open ponds ranged from − 3440 to 4198 μmol CO_2 m^{-2} h^{-1}. One open pond (O2) with dense aquatic vegetation took up CO_2 in summer, while winter measurements revealed consistent CO_2 release from all forest ponds (1414–2471 μmol CO_2 m^{-2} h^{-1}) and open ponds (330–3236 μmol CO_2 m^{-2} h^{-1}).

Maximum F_{CO2} in forest and open ponds in summer occurred at about 9:00, and the minimum at about 17:00, with both forest and open ponds showing a significant decline over the days (GAMM;

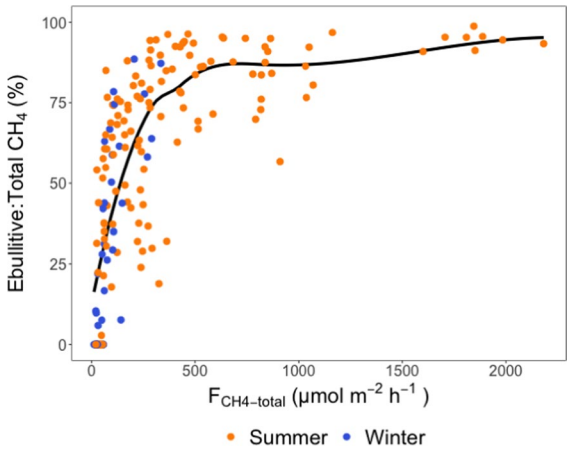

Fig. 4 Average $F_{CH4\text{-}total}$ plotted against average $F_{CH4\text{-}ebul}$: $F_{CH4\text{-}total}$ for each individual day for all ponds during summer and winter. Black line is fitted with a local polynomial regression model

forest: edf = 2, F = 45, $p < 0.001$, open: edf = 1.9, F = 26, $p < 0.001$, Fig. 5). A significant diel variation was also found during winter, in which higher fluxes were found in the evening or during the night, and lower fluxes during the day or early morning (GAMM; forest: edf = 1.9, F = 45, $p < 0.001$, open: edf = 1.9, F = 24, $p < 0.001$).

Drivers of CO_2 and CH_4 fluxes

Two models were fitted to each flux type, with the dependent variable being either hourly or daily fluxes (Table 3). Initially, all models included water temperature, oxygen concentration, sediment organic content (LOI), water depth, and plant coverage. R^2_{marg} was low for all hourly models (< 0.2), while R^2_{cond} was slightly higher (0.16–0.71), indicating that random effects accounted for some of the variation. The results from the ebullition model were particularly striking when daily rather than hourly values were used, increasing R^2 values of 0.11 and 0.34–0.17 and 0.68 for R^2_{marg} and R^2_{cond}, respectively. Both R^2_{marg} and R^2_{cond} were higher in the CH_4 models that applied average daily values, but this was not the case for R^2_{marg} in the CO_2 model. Oxygen was positively related to fluxes in the hourly CH_4 models, but not in the CO_2 model. When water depth was introduced in the final

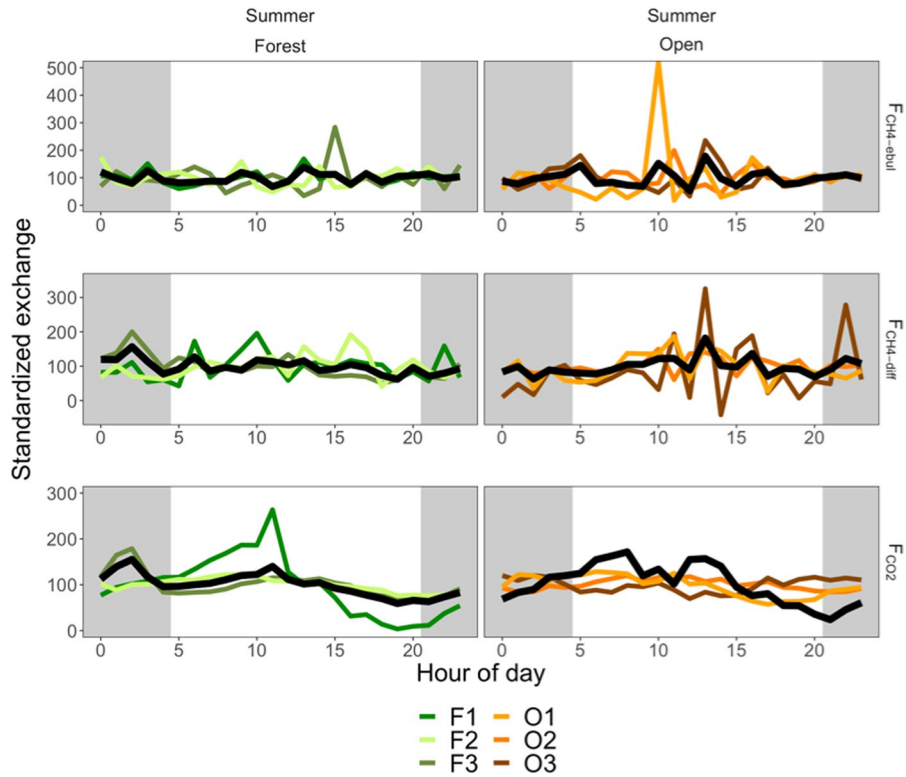

Fig. 5 Hourly standardized fluxes of forest and open ponds during summer of $F_{CH4\text{-}ebul}$, $F_{CH4\text{-}diff}$ and F_{CO2}. Black lines indicate the overall mean. Grey area indicates night hours

Table 3 Linear mixed effect models for CH_4 and CO_2 fluxes at hourly and daily scales at 4–6 sites and 6 ponds over several days in summer and winter. Estimates are scaled and centered, and can therefore be compared within each model

Dependent variable	Time resolution of variables	Parameters included	Estimates	R^2 Marginal|conditional
$F_{CH4\text{-}ebul}$	Hourly	LOI Oxygen concentration	− 105 110	0.11|0.34
$F_{CH4\text{-}diff}$	Hourly	LOI Water depth Oxygen concentration	21.8 11.1 7.3	0.08|0.16
F_{CO2}	Hourly	Water temperature* Oxygen concentration	134 − 808	0.03|0.71
$F_{CH4\text{-}ebul}$	Daily	LOI	− 189	0.17|0.68
$F_{CH4\text{-}diff}$	Daily	Plant coverage[a] Water temperature Ebullitive CH_4 exchange	− 22.7–133 − 13.8 − 19	0.34|0.47
F_{CO2}	Daily	Water temperature	673	0.02|0.91

[a]Plant coverage is a factorial variable and, thus, is estimated for each of the factors

*Parameters which showed a tendency ($0.05 < p < 0.1$)

model, it had a positive influence on the diffusive flux, while sediment organic content showed a negative correlation with daily $F_{CH4\text{-}ebul}$ and a positive correlation with $F_{CH4\text{-}diff}$. There were no obvious differences in fluxes with age or natural vs. human-made ponds, however, we only had a few ponds with little differences in age, thus more research is needed to evaluate the relationship.

Total greenhouse gas fluxes

On average, daily summer values of $F_{CH4\text{-}ebul}$ were 5.1-fold higher than $F_{CH4\text{-}diff}$ in forest ponds and 4.5-fold higher in open ponds (Table 2). During winter, the $F_{CH4\text{-}ebul}$:$F_{CH4\text{-}diff}$ ratios were around 1.0 in the forest (1) and open ponds (1.2).

The mean F_{CO2}:$F_{CH4\text{-}total}$ ratios (expressed in terms of moles) in forest and open ponds were lower in summer (5.5) than in winter (19.8 and 13.9, Table 2). The mean F_{CO2}:$F_{CH4\text{-}total}$ ratios in forest and open ponds expressed in terms of atmospheric warming potential were below 1.0 in summer (0.55 and 0.56) and above 1 during winter (2.0 and 1.4, Table 2). Thus, the warming potential of GHG fluxes was dominated by CH_4 during summer and by CO_2 during winter.

Discussion

Seasonal variations in CH_4 fluxes

Daily $F_{CH4\text{-}total}$ was sixfold higher during summer than winter in the small forest ponds and 3.9-fold higher in open ponds. However, winter fluxes were not negligible, while the increase of $F_{CH4\text{-}diff}$ from winter to summer was modest (1.5–twofold). Our findings suggest a marked increase in CH_4 formation at higher temperatures in the sediments, directly supporting ebullition, and only a relatively lower increase of diffusive CH_4 release of dissolved CH_4 in the pond water. The continued CH_4 release in winter agrees with data from more than 900 subarctic, boreal and temperate lakes and ponds showing CH_4 accumulation under winter ice despite low temperatures (< 4 °C; Denfeld et al. 2018a, b). However, despite low winter fluxes, Ollivier et al. (2019) showed that $F_{CH4\text{-}diff}$ in agricultural farm ponds increased 25-fold from winter to summer. An increase from winter to summer was observed in our data, but it was far less, most likely due to higher lability and amounts of the organic material entering the ponds with higher inflow in autumn and winter.

While $F_{CH4\text{-}ebul}$ at our sites declined substantially during winter, it remained higher than $F_{CH4\text{-}diff}$, likely because winter temperatures were not particularly low (mean: 9.4–9.9 °C). CH_4 bubbles are produced even

at very low temperatures under winter ice in lakes (Walter Anthony et al. 2010; Wik et al. 2011). Spatial variability of CH_4 ebullition is high and localized bubbles are often present in high densities trapped in the ice (Walter Anthony et al. 2010; Wik et al. 2011). High coefficients of variation generally indicated high spatiotemporal variability of CH_4 ebullition, both in this study and in an eutrophic lake examined previously (Sø et al. 2023a, b). Ebullitive release results from anaerobic degradation in the sediment and is not affected by dissolved CH_4 in the water column, but rather by sediment dissolved CH_4 concentration, the ambient pressure and the micro-environment (organic concent, sediment texture, production depth, etc.) where the bubbles are formed (Boudreau 2012). Previous studies have shown ebullitive events being primed by sudden drops in atmospheric pressure (Mattson & Likens 1990; Wik et al. 2013). In our study, however, we only observed modest daily changes in atmospheric pressure (0.1–3 Pa.), and only slightly higher during winter, which is why we did not test for an effect of pressure changes on ebullitive fluxes. The higher spatial variability of ebullition than diffusion of CH_4 is a general pattern also observed in other studies (Bastviken et al. 2004; Sø et al. 2023a, b; Yang et al. 2020).

Measurements of $F_{CH4\text{-}diff}$ were occasionally slightly negative, indicating an uptake of CH_4 from the floating chambers' headspace to the water. Similar results have been reported in areas with high plant cover or high oxygen concentrations (Miller et al. 2019; Sø et al. 2023a, b). While most of our negative fluxes occurred during winter in pond O3, which had a substantial winter plant cover, most of these negative values were close to the detection limit of the floating chambers. Also, when fluxes are close to zero, the error of the regression slope of CH_4 concentration *versus* time increases and negative values may occur by chance. Moreover, CH_4 uptake occurs if an inward gradient from air to pond surface is formed due to elevated atmospheric CH_4 concentration just above the ponds' surfaces and, thus, an elevated initial CH_4 concentration in the chamber's headspace after flushing. It is known that a dense, very active microbial neuston community is formed in a narrow $1-100$ µm layer immediately below pond surfaces, where CH_4 oxidation may take place (Conrad 1996).

Relationship between CO_2 and CH_4 fluxes

$F_{CH4\text{-}total}$ decreased more than F_{CO2} during winter, leading to a higher CO_2:CH_4 molar ratio during winter (open ponds = 13.9 and forest ponds = 19.8) than in summer (open = 5.5 and forest = 5.5). This may result from the lower temperature dependence (i.e., lower Q_{10} values and lower activation energy) of CO_2 formation than CH_4 formation (DelSontro et al. 2016; Jansen et al. 2020b; Yvon-Durocher et al. 2014). Importantly, CH_4 formation continued at low winter temperatures and should be addressed in the annual balances (Denfeld et al. 2018a; Karlsson et al. 2013). Quantification of winter F_{CO2} is even more important, as summer fluxes were only marginally higher than winter fluxes in small open ponds (ratio = 1.7) and appreciably lower in forest ponds (ratio = 1.5), where CO_2 was consumed by photosynthesis during summer, but less so during winter with lower solar radiation and temperatures. In our study, daily air temperature indicated that during 2022, similar temperature conditions like the ones we measured during winter (1–7 °C) occur almost one-third of the year (summer 32%), whereas mean solar radiation similar to our winter measurements (0–80 W m^{-2}) occurred almost 50% of the year (summer 48%).

Pathways of CH_4 fluxes

In summer and winter comparisons among all sites in the six ponds higher $F_{CH4\text{-}diff}$ was accompanied by even higher $F_{CH4\text{-}ebul}$. Thus, the proportion of $F_{CH4\text{-}ebul}$ increased from zero at low total CH_4 release to more than 90% of $F_{CH4\text{-}total}$, in accordance with our hypothesis. A likely explanation is that the diffusive CH_4 release across the sediment surface only keeps pace with a modest CH_4 production rate. However, when CH_4 production increases at high temperatures, CH_4 concentrations build up and bubbles are formed and released, bypassing possible oxidation in an oxic sediment surface and water column (Langenegger et al. 2019). This pattern was noticeable in our dataset as the summer $F_{CH4\text{-}total}$ were generally higher than winter total CH_4 emission, most likely a result of the increased CH_4 production at higher temperature. While bubble release is limited mainly by the rate of CH_4 production and physical restraints before being released from the sediment (Wik et al. 2013, 2018), diffusive flux is constrained by several biological and

physical processes, including oxidation in surface sediments and water column, and low gas transfer velocities at the sediment–water and air–water interface (Bastviken 2009). Our initial models showed a significant relationship with meteorological variables; however, this relationship vanished when differentiating between seasons, which suggests that it was caused by coupled differences in CH_4 and meteorological variables between summer and winter.

Diel variations in CO_2 and CH_4 fluxes

The automated floating chambers measure GHG fluxes every hour and are particularly suited to detect possible diel patterns. In summer, $F_{CH4\text{-}diff}$ was significantly higher in the early morning than during the evening in forest ponds possibly related to convective mixing, as the ponds do not stratify and the air might become colder than the water during the night (Podgrajsek et al. 2014). In open ponds, a maximum was seen around noon, which correlated well with increasing wind speeds. Maximum F_{CO2} in forest ponds in summer occurred late in the morning following nighttime respiration, and the minimum was observed late in the afternoon after extended daytime photosynthesis. Our diel patterns show similar results to those of Miller et al. (2019) who found that diel fluxes of CH_4 and CO_2 from drawdown ponds can vary widely throughout the day while being dependent on water temperature, hour of the day, pH and oxygen concentration.

Overall, the diel variability of $F_{CH4\text{-}diff}$ was not nearly as pronounced as that observed in larger lakes, where wind exposure and gas transfer velocities are higher (Sieczko et al. 2020). If diel patterns observed in previous literature (Rudberg et al. 2021; Sieczko et al. 2020) are driven by wind shear and variable gas transfer velocities, open ponds may exert a more pronounced diel pattern as they are more susceptible to wind due to the lack of terrestrial sheltering. However, our results indicate lower CH_4 fluxes in open ponds, which could restrict the detection of diel patterns because variability was low. By contrast, $F_{CH4\text{-}ebul}$ is a highly stochastic process independent of wind day and night and, as anticipated, it did not vary systematically during the diel cycle.

CO_2 is consumed in the water by daytime photosynthesis and commonly changes CO_2 uptake from the atmosphere to nocturnal release (Martinsen et al. 2022). Thus, when both CO_2 and CH_4 are measured in freshwater habitats, it is essential to include measurements during both day and night as gas flux often exhibits profound diel variability related to the influence of solar radiation on photosynthesis, temperature, and ventilated gas flow of CO_2 and CH_4 through floating-leaved plants (Brix et al. 1992; Dacey & Klug 1979; Martinsen et al. 2022).

Pond greenhouse gas fluxes

Combined, F_{CO2} and $F_{CH4\text{-}total}$ showed a significant carbon loss from ponds and a high warming potential. Assuming that the mean of summer and winter fluxes is a fair measure of annual fluxes, they attained 2453 g CO_2e m^{-2} y^{-1} from the forest ponds and less, 911 g CO_2e m^{-2} y^{-1}, from the open ponds (Table 2). A higher mean carbon flux (i.e., 6600 g CO_2e m^{-2}) was calculated from several small ponds (< 1000 m^2); however, these values are tied to large uncertainties in CH_4 fluxes (Holgerson & Raymond 2016; Rosentreter et al. 2021). These ponds with very large carbon flux resemble phytoplankton primary productivity in nutrient-rich lakes (Kalff & Knoechel 1978), reflecting the high input of terrestrial and in-pond production of organic material (Mulholland & Elwood 1982).

The annual global warming potential (GWP) of released CH_4 was comparable to that of CO_2, representing 60% of the combined GWP of both gases in the studied forest ponds, 44% in the open ponds, and, in comparison, 37% as the average of < 1000 m^2 ponds compiled by Holgerson and Raymond (2016). Previous research have shown a change in GHG emissions from ponds of different age and type (natural vs. artificial) (Abril et al. 2005; Goeckner et al. 2022; Phyoe & Wang 2019), but this was not observed for our ponds. Our ponds were mostly created to restore the natural hydrology rather than digging holes, as the artificial ponds examined by Goeckner et al. (2022) were. An initial outburst of GHG emission could be expected when sites are inundated, but our ponds are many years old and if they had experienced an initial outburst, we are likely far beyond the relevant time to measure this. On the other hand, our forest ponds might not have decreased in emissions over time due to the substantial terrestrial input they receive.

In discussions of GHG, it has been pointed out, that the re-establishment of small lakes and ponds leads to a substantial release of CO_2 and CH_4 to the atmosphere (Goeckner et al. 2022; Pi et al. 2022). CO_2 and CH_4 release is a natural consequence of the high terrestrial input of organic carbon and supersaturated CO_2 relative to pond surfaces. In carbon budget evaluations, it is necessary to account for the permanent burial of organic carbon in pond sediments (Sand-Jensen & Staehr 2012). Furthermore, the origin of the carbon is important, as autochthonous carbon does not remove external carbon, which would be the case when the inputs are allochthonous (Prairie et al. 2018). However, due to the surroundings, we expect the carbon input to be primarily allochthonous in the measured ponds, although this was not tested. Annual sedimentation rates for nine small eutrophic Danish lakes as a function of maximum water depth (Anderson et al. 2014) suggest a sedimentation rate of about 550 g CO_2e m^{-2} y^{-1} by extrapolation to a water depth of 1 m, typical of the ponds studied here. Direct measurements performed by digging out the organic material accumulated over a few years after the establishment of ponds in the English countryside yielded annual rates of 290–906 g CO_2e m^{-2} y^{-1} (Taylor et al. 2019). Other studies have found rates varying from 29 to 1638 g CO_2e m^{-2} y^{-1} (Goeckner et al. 2022; Ljung & Lin 2023). Though we assume that annual accumulation in small ponds is in the upper part of this range due to the high terrestrial input and the gradual expansion of littoral plants across the water surface, ultimately turning ponds into moors and bogs (Wetzel 1983), we apply a conservative mean annual sediment accumulation of 550 g CO_2e m^{-2}. We compared the resulting warming potential of ponds with that of drained cropland, drained unutilized land, and rewetted soils (Tiemeyer et al. 2020) that are commonly converted to ponds to increase local biodiversity and reduce downstream eutrophication and flooding risk (Schmadel et al. 2019). If estimated organic matter deposition in our ponds and measured GHG fluxes are accounted for, the annual GWP of open ponds is low (361 g CO_2e m^{-2} y^{-1}; Table 4), while that of forest ponds is higher (1903 g CO_2e m^{-2} y^{-1}). The annual GWP of rewetted organic soils (686 g CO_2e m^{-2}) resembles that of open ponds, while drained cropland and uncultivated wetland on organic soils have much higher warming potentials (3718 and 2799 g CO_2e m^{-2}) than both our pond types.

Table 4 Annual warming potential of CO_2, CH_4, and N_2O exchange from three types of wetlands in Germany (Tiemeyer et al. 2020, their Table 2) compared to that of small Danish ponds in this study

Ecosystem type	CO_2	CH_4	N_2O	Sedimentation	SUM
Croplands	3373	13.8	330.8	0	3718
Drained unutilized land	2603	175	20.9	0	2799
Rewetted organic soil	−15	697.5	2.98	0	686
Forest ponds	1057	1397	0	−550	1903
Open ponds	385	526	0	−550	361

Temperatures and landscapes studied in Germany resemble Danish conditions. All values in g CO_2e m^{-2} y^{-1}. N_2O emission is assumed to be 0 in the ponds due to very low nitrate concentrations (Table 1), while sedimentation is only expected to occur in the ponds

The deep sediment cores (5–10 cm, data not shown) were expected to portray the surrounding soils, which in all forest ponds showed organic contents higher than 20%, while in open ponds organic content was from 10.1, 5.3 and 11.4%, the lowest content was in the deepest of ponds, which was artificially dug. We therefore believe that the comparison with Tiemeyer et al. (2020) is appropriate, as their estimation is based on organic-rich soils (12–18% C; IPCC 2006).

Conversion of drained cultivated and uncultivated organic soils to wetlands and ponds shifts organic carbon degradation into carbon retention and, though more CH_4 is released, the carbon, nitrogen, and phosphorus retention in pond sediment and the reduction of N_2O fluxes when the addition of nitrogen fertilizers ceases will markedly reduce the warming potential. In conclusion, to establish a fair evaluation of conservation and management initiatives to form new ponds to replace the many lost it is essential to account for overall GHG budgets, biodiversity and downstream eutrophication and flooding risk. We propose that everyone will benefit from the conversion of drained cultivated organic soils into natural wetlands or ponds.

Acknowledgements We thank the Independent Research Fund Denmark (0217-00112B) for supporting the project "Supporting climate and biodiversity by rewetting low-lying areas" to KSJ. Furthermore, we thank Aage V. Jensens's foundation for grants supporting the Ph.D. research of JSS. We thank the COWI foundation for funding CH_4 sensors (A-155.03) and the Carlsberg grant for funding the Ultraportable Greenhouse

Gas Analyzer (CF21-0166). We thank David Stuligross for proof-reading the manuscript and Johan Emil Kjær for field assistance.

Author contribution The conceptualization of the project was done by all authors, with JSS, TK, and KSJ developing the idea of this project. Equipment was developed by JSS and TK. The investigation was done by JSS, TK, and KTM, while the formal analysis and visualization were performed by JSS and KTM. KSJ and JSS wrote the original draft, while all authors contributed to the reviewing and editing. Funding acquisition was done by TK and KSJ.

Funding Open access funding provided by University of Southern Denmark.

Data availability All data are made available from an online repository using the following link: https://doi.org/https://doi.org/10.5281/zenodo.8091055 (Sø et al. 2023a, b).

Declarations

Conflict of interest The authors declare no known competing interests.

References

Abril G, Borges AV (2019) Ideas and perspectives: carbon leaks from flooded land: do we need to replumb the inland water active pipe? Biogeosciences 16(3):769–784. https://doi.org/10.5194/bg-16-769-2019

Abril G, Guérin F, Richard S, Delmas R, Galy-Lacaux C, Gosse P, Matvienko B (2005) Carbon dioxide and methane emissions and the carbon budget of a 10-year old tropical reservoir (Petit Saut, French Guiana). Glob Biogeochem Cycles 19(4) https://doi.org/10.1029/2005GB002457

Anderson NJ, Bennion H, Lotter AF (2014) Lake eutrophication and its implications for organic carbon sequestration in Europe. Glob Change Biol 20(9):2741–2751. https://doi.org/10.1111/gcb.12584

Bartoń K (2018) MuMIn: multi-model inference (Version R package version 1.42.1). Retrieved from https://CRAN.R-project.org/package=MuMIn

Bastviken D (2009) Methane. In: Likens GE (ed) Encyclopedia of inland waters. Academic Press, Oxford, pp 783–805

Bastviken D, Cole J, Pace M, Tranvik L (2004) Methane emissions from lakes: dependence of lake characteristics, two regional assessments, and a global estimate. Glob Biogeochem Cycl. https://doi.org/10.1029/2004gb002238

Bastviken D, Sundgren I, Natchimuthu S, Reyier H, Gålfalk M (2015) Technical note: cost-efficient approaches to measure carbon dioxide (CO_2) fluxes and concentrations in terrestrial and aquatic environments using mini loggers. Biogeosciences 12(12):3849–3859. https://doi.org/10.5194/bg-12-3849-2015

Bastviken D, Nygren J, Schenk J, Parellada Massana R, Duc NT (2020) Technical note: facilitating the use of low-cost methane (CH_4) sensors in flux chambers – calibration, data processing, and an open-source make-it-yourself logger. Biogeosciences 17(13):3659–3667. https://doi.org/10.5194/bg-17-3659-2020

Bates D, Maechler M, Bolker B, Walker S (2015) Fitting linear mixed-effects models using lme4. J Stat Softw 67(1):1–48

Beaulieu JJ, DelSontro T, Downing JA (2019) Eutrophication will increase methane emissions from lakes and impoundments during the 21st century. Nat Commun 10(1):1375. https://doi.org/10.1038/s41467-019-09100-5

Bogard MJ, Kuhn CD, Johnston SE, Striegl RG, Holtgrieve GW, Dornblaser MM, Butman DE (2019) Negligible cycling of terrestrial carbon in many lakes of the arid circumpolar landscape. Nat Geosci 12(3):180–185

Boudreau BP (2012) The physics of bubbles in surficial, soft, cohesive sediments. Mar Pet Geol 38(1):1–18

Brix H, Sorrell BK, Orr PT (1992) Internal pressurization and convective gas flow in some emergent freshwater macrophytes. Limnol Oceanogr 37(7):1420–1433

Céréghino R, Boix D, Cauchie H-M, Martens K, Oertli B (2014) The ecological role of ponds in a changing world. Hydrobiologia 723(1):1–6. https://doi.org/10.1007/s10750-013-1719-y

Conrad R (1996) Soil microorganisms as controllers of atmospheric trace gases (H_2, CO, CH_4, OCS, N_2O, and NO). Microbiol Rev 60(4):609–640. https://doi.org/10.1128/mr.60.4.609-640.1996

Dacey J, Klug M (1979) Methane efflux from lake sediments through water lilies. Science 203(4386):1253–1255

D'Ambrosio SL, Harrison JA (2021) Methanogenesis exceeds CH_4 consumption in eutrophic lake sediments. Limnol Oceanogr Lett 6(4):173–181. https://doi.org/10.1002/lol2.10192

Deemer BR, Holgerson MA (2021) Drivers of methane flux differ between lakes and reservoirs, complicating global upscaling efforts. J Geophys Res Biogeosci 126(4):e2019JG005600. https://doi.org/10.1029/2019JG005600

Deemer BR, Harrison JA, Li S, Beaulieu JJ, DelSontro T, Barros N, Vonk JA (2016) Greenhouse gas emissions from reservoir water surfaces: a new global synthesis. Bioscience 66(11):949–964. https://doi.org/10.1093/biosci/biw117

DelSontro T, Boutet L, St-Pierre A, del Giorgio PA, Prairie YT (2016) Methane ebullition and diffusion from northern ponds and lakes regulated by the interaction between temperature and system productivity. Limnol Oceanogr 61(S1):S62–S77

Denfeld BA, Baulch HM, Giorgio PAd, Hampton SE, Karlsson J (2018a) A synthesis of carbon dioxide and methane dynamics during the ice-covered period of northern lakes. Limnol Oceanogr Lett 3(3):117–131. https://doi.org/10.1002/lol2.10079

Denfeld BA, Klaus M, Laudon H, Sponseller RA, Karlsson J (2018b) Carbon dioxide and methane dynamics in a small boreal lake during winter and spring melt events. J Geophys Res Biogeosci 123(8):2527–2540

Dibike Y, Prowse T, Saloranta T, Ahmed R (2011) Response of Northern Hemisphere lake-ice cover and lake-water thermal structure patterns to a changing climate. Hydrol Process 25(19):2942–2953. https://doi.org/10.1002/hyp.8068

Donis D, Flury S, Stöckli A, Spangenberg JE, Vachon D, McGinnis DF (2017) Full-scale evaluation of methane production under oxic conditions in a mesotrophic lake. Nat Commun 8(1):1–12

Duc NT, Crill P, Bastviken D (2010) Implications of temperature and sediment characteristics on methane formation and oxidation in lake sediments. Biogeochemistry 100(1):185–196

Eugster W, Laundre J, Eugster J, Kling GW (2020) Long-term reliability of the Figaro TGS 2600 solid-state methane sensor under low-Arctic conditions at Toolik Lake. Alaska Atmos Meas Tech 13(5):2681–2695. https://doi.org/10.5194/amt-13-2681-2020

Fenchel T, Blackburn H, King GM, Blackburn TH (2012) Bacterial biogeochemistry: the ecophysiology of mineral cycling. Academic press

Gilbert PJ, Taylor S, Cooke DA, Deary ME, Jeffries MJ (2021) Quantifying organic carbon storage in temperate pond sediments. J Environ Manage 280:111698. https://doi.org/10.1016/j.jenvman.2020.111698

Goeckner AH, Lusk MG, Reisinger AJ, Hosen JD, Smoak JM (2022) Florida's urban stormwater ponds are net sources of carbon to the atmosphere despite increased carbon burial over time. Commun Earth Environ 3(1):53. https://doi.org/10.1038/s43247-022-00384-y

Grinham A, Albert S, Deering N, Dunbabin M, Bastviken D, Sherman B, Evans CD (2018) The importance of small artificial water bodies as sources of methane emissions in Queensland Australia. Hydrol Earth Syst Sci 22(10):5281–5298. https://doi.org/10.5194/hess-22-5281-2018

Holgerson MA, Raymond PA (2016) Large contribution to inland water CO_2 and CH_4 emissions from very small ponds. Nat Geosci 9(3):222–226

IPCC (2022) Climate change 2022: impacts. Cambridge University Press, Adaptation and Vulnerability

IPCC (2006) IPCC guidelines for national greenhouse gas inventories: OECD

Jansen J, Thornton BF, Cortés A, Snöälv J, Wik M, MacIntyre S, Crill PM (2020a) Drivers of diffusive CH_4 emissions from shallow subarctic lakes on daily to multi-year timescales. Biogeosciences 17(7):1911–1932

Jansen J, Thornton BF, Wik M, MacIntyre S, Crill PM (2020b) Temperature proxies as a solution to biased sampling of lake methane emissions. Geophys Res Lett 47(14):e2020GL088647. https://doi.org/10.1029/2020GL088647

Jespersen A-M, Christoffersen K (1987) Measurements of chlorophyll-a from phytoplankton using ethanol as extraction solvent. Arch Hydrobiol 109(3):445–454

Joyce J, Jewell PW (2003) Physical controls on methane ebullition from reservoirs and lakes. Environ Eng Geosci 9(2):167–178

Kajiura M, Tokida T (2021) Quantifying bubbling emission (ebullition) of methane from a rice paddy using high-time-resolution concentration data obtained during a closed-chamber measurement. J Agric Meteorol. https://doi.org/10.21203/rs.3.rs-396475/v1

Kalff J, Knoechel R (1978) Phytoplankton and their dynamics in oligotrophic and eutrophic lakes. Annu Rev Ecol Syst 9:475–495

Karlsson J, Giesler R, Persson J, Lundin E (2013) High emission of carbon dioxide and methane during ice thaw in high latitude lakes. Geophys Res Lett 40(6):1123–1127. https://doi.org/10.1002/grl.50152

Kirk JT (1994) Light and photosynthesis in aquatic ecosystems. Cambridge University Press

Kragh T, Søndergaard M (2004) Production and bioavailability of autochthonous dissolved organic carbon: effects of mesozooplankton. Aquat Microb Ecol 36(1):61–72

Kuhn MA, Varner RK, Bastviken D, Crill P, MacIntyre S, Turetsky M, Olefeldt D (2021) BAWLD-CH4: a comprehensive dataset of methane fluxes from boreal and arctic ecosystems. Earth Syst Sci Data 13(11):5151–5189

Lammirato C, Lebender U, Tierling J, Lammel J (2017) Analysis of uncertainty for N_2O fluxes measured with the closed chamber method under field conditions: calculation method, detection limit and spatial variability. J Plant Nutr Soil Sci. https://doi.org/10.1002/jpln.201600499

Langenegger T, Vachon D, Donis D, McGinnis DF (2019) What the bubble knows: lake methane dynamics revealed by sediment gas bubble composition. Limnol Oceanogr 64(4):1526–1544

Laurion I, Vincent WF, MacIntyre S, Retamal L, Dupont C, Francus P, Pienitz R (2010) Variability in greenhouse gas emissions from permafrost thaw ponds. Limnol Oceanogr 55(1):115–133. https://doi.org/10.4319/lo.2010.55.1.0115

Ljung K, Lin S (2023) Organic carbon burial in constructed ponds in southern Sweden. Earth Sci Syst Soc. https://doi.org/10.3389/esss.2023.10061

Lyngvig R (2022) The weather of Hillerød. Retrieved from https://www.hilleroed-vejr.dk. Accessed on November 23, 2022

Martinsen KT, Kragh T, Sand-Jensen K (2018) Technical note: a simple and cost-efficient automated floating chamber for continuous measurements of carbon dioxide gas flux on lakes. Biogeosciences 15(18):5565–5573. https://doi.org/10.5194/bg-15-5565-2018

Martinsen KT, Zak NB, Baastrup-Spohr L, Kragh T, Sand-Jensen K (2022) Ecosystem metabolism and gradients of temperature, oxygen and dissolved inorganic carbon in the littoral zone of a macrophyte-dominated lake. J Geophys

Res Biogeosci 127(12):e2022JG007193. https://doi.org/10.1029/2022JG007193
Mattson MD, Likens GE (1990) Air pressure and methane fluxes. Nature 347(6295):718–719. https://doi.org/10.1038/347718b0
Miller BL, Chen H, He Y, Yuan X, Holtgrieve GW (2019) Magnitudes and drivers of greenhouse gas fluxes in floodplain ponds during drawdown and inundation by the three gorges reservoir. J Geophys Res Biogeosci 124(8):2499–2517. https://doi.org/10.1029/2018JG004701
Mulholland PJ, Elwood JW (1982) The role of lake and reservoir sediments as sinks in the perturbed global carbon cycle. Tellus 34(5):490–499
Myhre G, Shindell D (2014) Anthropogenic and natural radiative forcing. In C. Intergovernmental panel on climate (ed.), Climate change 2013—the physical science basis: working group I contribution to the fifth assessment report of the intergovernmental panel on climate change (pp 659–740). Cambridge: Cambridge University Press
Ollivier QR, Maher DT, Pitfield C, Macreadie PI (2019) Winter emissions of CO2, CH4, and N_2O from temperate agricultural dams: fluxes, sources, and processes. Ecosphere 10(11):e02914. https://doi.org/10.1002/ecs2.2914
Peacock M, Audet J, Bastviken D, Cook S, Evans CD, Grinham A, Futter MN (2021) Small artificial waterbodies are widespread and persistent emitters of methane and carbon dioxide. Glob Change Biol 27(20):5109–5123. https://doi.org/10.1111/gcb.15762
Phyoe WW, Wang F (2019) A review of carbon sink or source effect on artificial reservoirs. Int J Environ Sci Technol 16(4):2161–2174. https://doi.org/10.1007/s13762-019-02237-2
Pi X, Luo Q, Feng L, Xu Y, Tang J, Liang X, Bryan BA (2022) Mapping global lake dynamics reveals the emerging roles of small lakes. Nat Commun 13(1):5777. https://doi.org/10.1038/s41467-022-33239-3
Podgrajsek E, Sahlée E, Rutgersson A (2014) Diurnal cycle of lake methane flux. J Geophys Res Biogeosci 119(3):236–248
Prairie YT, Alm J, Beaulieu J, Barros N, Battin T, Cole J, Vachon D (2018) Greenhouse gas emissions from freshwater reservoirs what does the atmosphere see? Ecosystems 21(5):1058–1071
R Core Team (2018) R: a language and environment for statistical computing. Retrieved from https://www.R-project.org/
Richardson DC, Holgerson MA, Farragher MJ, Hoffman KK, King KBS, Alfonso MB, Sweetman JN (2022) A functional definition to distinguish ponds from lakes and wetlands. Sci Rep 12(1):10472. https://doi.org/10.1038/s41598-022-14569-0
Riera JL, Schindler JE, Kratz TK (1999) Seasonal dynamics of carbon dioxide and methane in two clear-water lakes and two bog lakes in northern Wisconsin, U.S.A. Can J Fish Aquat Sci 56(2):265–274. https://doi.org/10.1139/f98-182
Rosentreter JA, Borges AV, Deemer BR, Holgerson MA, Liu S, Song C, Eyre BD (2021) Half of global methane emissions come from highly variable aquatic ecosystem sources. Nat Geosci 14(4):225–230. https://doi.org/10.1038/s41561-021-00715-2
Rudberg D, Duc N, Schenk J, Sieczko A, Pajala G, Sawakuchi HO, Karlsson J (2021) Diel variability of CO_2 emissions from northern lakes. J Geophys Res Biogeosci 126(10):e2021JG006246
Sand-Jensen K, Staehr PA (2009) Net heterotrophy in small danish lakes: a widespread feature over gradients in trophic status and land cover. Ecosystems 12(2):336–348. https://doi.org/10.1007/s10021-008-9226-0
Sand-Jensen K, Staehr PA (2012) CO_2 dynamics along Danish lowland streams: water–air gradients, piston velocities and evasion rates. Biogeochemistry 111(1):615–628. https://doi.org/10.1007/s10533-011-9696-6
Sand-Jensen K, Andersen MR, Martinsen KT, Borum J, Kristensen E, Kragh T (2019) Shallow plant-dominated lakes – extreme environmental variability, carbon cycling and ecological species challenges. Ann Bot 124(3):355–366. https://doi.org/10.1093/aob/mcz084
Schmadel NM, Harvey JW, Schwarz GE, Alexander RB, Gomez-Velez JD, Scott D, Ator SW (2019) Small ponds in headwater catchments are a dominant influence on regional nutrient and sediment budgets. Geophys Res Lett 46(16):9669–9677. https://doi.org/10.1029/2019GL083937
Sieczko AK, Duc NT, Schenk J, Pajala G, Rudberg D, Sawakuchi HO, Bastviken D (2020) Diel variability of methane emissions from lakes. Proc Natl Acad Sci 117(35):21488–21494. https://doi.org/10.1073/pnas.2006024117
Sø JS, Sand-Jensen K, Martinsen KT, Polauke E, Kjær JE, Reitzel K, Kragh T (2023a) Methane and carbon dioxide fluxes at high spatiotemporal resolution from a small temperate lake. Sci Total Environ 878:162895. https://doi.org/10.1016/j.scitotenv.2023.162895
Sø, J. S., Martinsen, K. T., Kragh, T., & Sand-Jensen, K. (2023). JonasStage/seasonal_pond_ghg: v1.0.0. Retrieved from: https://doi.org/10.5281/zenodo.8091055
Striegl RG, Michmerhuizen CM (1998) Hydrologic influence on methane and carbon dioxide dynamics at two north-central Minnesota lakes. Limnol Oceanogr 43(7):1519–1529. https://doi.org/10.4319/lo.1998.43.7.1519
Taylor S, Gilbert PJ, Cooke DA, Deary ME, Jeffries MJ (2019) High carbon burial rates by small ponds in the landscape. Front Ecol Environ 17(1):25–31. https://doi.org/10.1002/fee.1988
Tiemeyer B, Freibauer A, Borraz EA, Augustin J, Bechtold M, Beetz S, Drösler M (2020) A new methodology for organic soils in national greenhouse gas inventories: data synthesis, derivation and application. Ecol Indic 109:105838. https://doi.org/10.1016/j.ecolind.2019.105838
Vachon D, Prairie YT (2013) The ecosystem size and shape dependence of gas transfer velocity versus wind speed relationships in lakes. Can J Fish Aquat Sci 70(12):1757–1764
Walter Anthony KM, Vas DA, Brosius L, Chapin FS III, Zimov SA, Zhuang Q (2010) Estimating methane emissions from northern lakes using ice-bubble surveys. Limnol Oceanogr Methods 8(11):592–609
West WE, Creamer KP, Jones SE (2016) Productivity and depth regulate lake contributions to atmospheric methane. Limnol Oceanogr 61(S1):S51–S61

Wetzel RG (1983) Limnology, 2nd edn. Saunders, Philadelphia
Wik M, Crill PM, Varner RK, Bastviken D (2013) Multiyear measurements of ebullitive methane flux from three subarctic lakes. J Geophys Res Biogeosci 118(3):1307–1321. https://doi.org/10.1002/jgrg.20103
Wik M, Thornton BF, Bastviken D, MacIntyre S, Varner RK, Crill PM (2014) Energy input is primary controller of methane bubbling in subarctic lakes. Geophys Res Lett 41(2):555–560. https://doi.org/10.1002/2013GL058510
Wik M, Johnson JE, Crill PM, DeStasio JP, Erickson L, Halloran MJ, Varner RK (2018) Sediment characteristics and methane ebullition in three subarctic lakes. J Geophys Res Biogeosci 123(8):2399–2411
Wik M, Crill PM, Bastviken D, Danielsson Å, Norbäck E (2011) Bubbles trapped in arctic lake ice: potential implications for methane emissions. J Geophys Res Biogeosci 116(G3)
Wood S (2011) Fast stable restricted maximum likelihood and marginal likelihood estimation of semiparametric generalized linear models. J Royal Stat Soc (B). Retrieved from http://cran.r-project.org/web/packages/mgcv/index.html
Yang P, Zhang Y, Yang H, Guo Q, Lai DY, Zhao G, Tong C (2020) Ebullition was a major pathway of methane emissions from the aquaculture ponds in southeast China. Water Res 184:116176. https://doi.org/10.1016/j.watres.2020.116176
Yvon-Durocher G, Allen AP, Bastviken D, Conrad R, Gudasz C, St-Pierre A, Del Giorgio PA (2014) Methane fluxes show consistent temperature dependence across microbial to ecosystem scales. Nature 507(7493):488–491. https://doi.org/10.1038/nature13164